



Joint charging scheduling of electric buses and active power flexibility integration

Downloaded from: <https://research.chalmers.se>, 2025-04-04 07:04 UTC

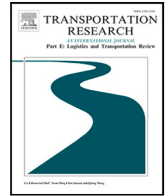
Citation for the original published paper (version of record):

Najafi, A., Gao, K., Wang, H. et al (2025). Joint charging scheduling of electric buses and active power flexibility integration. *Transportation Research Part E: Logistics and Transportation Review*, 197(104038). <http://dx.doi.org/10.1016/j.tre.2025.104038>

N.B. When citing this work, cite the original published paper.

Contents lists available at [ScienceDirect](https://www.sciencedirect.com)

Transportation Research Part E

journal homepage: www.elsevier.com/locate/tre

Joint charging scheduling of electric buses and active power flexibility integration[☆]

Arsalan Najafi^{a,b}, Kun Gao^{a,*}, Hua Wang^{c,*}, Michal Jasinski^b, Omkar Parishwad^a, Shaohua Cui^a, Xiaohan Liu^a

^a Department of Architecture and Civil Engineering, Chalmers University of Technology, Goteburg SE 41296, Sweden

^b Department of Electrical Engineering Fundamentals, Wroclaw University of Science and Technology, 50-370 Wroclaw, Poland

^c School of Automotive and Transportation Engineering, Hefei University of Technology, Hefei, 230009, China

ARTICLE INFO

Keywords:

Battery electric bus
Active distribution network
Coupled transportation and power networks
Demand response
Stochastic programming

ABSTRACT

Public transport electrification stands out as a notable response to the environmental concerns in the transport sector. This study proposes a joint optimization framework for the coupled battery electric bus (BEB) transit system and active power distribution network (APDN) integrated with the flexibility of demand response (DR). The primary objective is to effectively support BEB mobility services by addressing their spatial and temporal charging demands. Special emphasis is placed on leveraging APDN capabilities to facilitate BEB operations with minimal costs. The problem is formulated as a bi-level stochastic programming by incorporating the non-profit agent at the upper level and the DR aggregators at the lower level. The upper level aims to minimize the joint costs of the APDN and BEB transit system, while the lower level seeks to maximize its profit through interaction with the upper level. The problem is then reformulated into an equivalent single-level model using Karush–Kuhn–Tucker conditions. The findings underscore the effective coupling framework in tackling the charging scheduling in the BEB sub-transit system in Skövde, Sweden, alongside the proper DR activation to meet the technical constraints of the coupled BEB transit and APDN. The proposed optimization framework can compensate for the additional burden of charging demands from BEBs by curtailing 6.4% of energy during peak hours.

1. Introduction

The electric transportation system has garnered significant attention in recent years due to the needs of reduction in global greenhouse gas emissions. Expanding public transport electrification stands out as a notable response to the environmental concerns in the transport sector (He et al., 2023; Zhou et al., 2024b). Battery electric buses (BEBs) have attracted considerable attention due to their benefits such as low emissions and enhanced energy efficiency (Wang et al., 2017; Zhang et al., 2023). However, despite these advantages, the integration of BEBs into existing urban transport systems poses significant challenges. For example, the higher upfront cost of BEBs compared to fuel-based buses hinders their widespread adoption and efficient operation

[☆] The research is supported by the research grant from National Natural Science Foundation Council of China (No. 72471070), JPI Urban Europe and Energimyndigheten (e-MATS, P2023-00029), and Area of Advance Transport at Chalmers University of Technology. Any opinions, findings, and conclusions or recommendations expressed in this paper are those of the authors and do not necessarily reflect the views of the sponsors.

* Correspondence to: Sven Hultins Gata, 41296, Gothenborg, Sweden.

E-mail addresses: gkun@chalmers.se (K. Gao), hwang191901@hfut.edu.cn (H. Wang).

<https://doi.org/10.1016/j.tre.2025.104038>

Received 24 July 2024; Received in revised form 14 February 2025; Accepted 15 February 2025

Available online 3 March 2025

1366-5545/© 2025 The Authors. Published by Elsevier Ltd. This is an open access article under the CC BY license (<http://creativecommons.org/licenses/by/4.0/>).

Nomenclature

A. Sets and indices:

t, \mathcal{T}	Index and set of timeslots.
w, \mathcal{W}	Index and set of scenarios.
k, \mathcal{G}	Index and set of DR aggregators.
b, \mathcal{B}	Index and set of nodes in active power distribution network.
n, \mathcal{N}	Index and set of nodes of the BEB transit system.
\mathcal{B}^N	Set of electrified nodes in APDN.
\mathcal{B}^G	Set of APDN nodes which are managed by aggregators.
i, j, \mathcal{S}	Indices and set of service trips in transit system.
o, \mathcal{O}	Index and set of the first trips departing the depot.
d, \mathcal{D}	Index and set of the last trips arriving at the depot.
\mathcal{OS}	Set of all trips excluding the last trips to the depot.
\mathcal{SD}	Set of all trips excluding the first trips leaving the depot.

B. Parameters:

$D_{b,t}^P, D_{b,t}^Q$	Active and reactive loads of APDN at node b at t .
$\lambda_{t,w}^M$	Electricity market price at scenario w .
λ^{BEB}	Procurement price of BEBs.
λ_b^{NS}	Price of energy not supplied at APDN node b .
M_1, M_2	Big numbers.
Φ_b	Coefficient of power curtailment at APDN node b .
A_b	Coefficient of energy curtailment at APDN node b .
$c_{b,t}^{\text{DR}}$	Incentive price of load curtailment at node b .
r_b, x_b	Resistance and reactance of branch $b, b + 1$ in APDN.
\bar{V}, \underline{V}	Upper and lower bound of output voltage.
$\bar{P}_{b,w}^{\text{PV}}$	Maximum generation limit of PV panel at node b , scenario w and time t .
ρ_w	Probability of scenario w .
PF	Penalty factor of voltage deviation from the minimum limit.
u_i, \bar{u}_i	Start and end time of service trip i .
τ_{ij}^{S2D}	Deadhead trip time from service trip i to depots ($j \in \mathcal{D}$).
τ_i^{O2S}	Deadhead trip time from the origin node (depot) to trip i .
τ_i^{DH}	Deadhead trip time upon finishing trip i .
τ_i	Travel time of service trip i .
\underline{Y}, \bar{Y}	Minimum and maximum battery energy percentage.
A	Capacity of a BEB.
c_{oi}^{O2S}	Energy consumption from the depot to initiate the first service trip.
c_i^{SL}	Energy consumption during service trip i .
c_{ij}^{S2D}	Energy consumption upon finishing the last trip and arriving at the depot ($j \in \mathcal{D}$).
c_{ij}^{ST}	Energy consumption after trip i and before trip j .
\mathbb{I}_{bg}	A binary input to define whether consumer b is registered through aggregator g .
p_n^{EnMax}	Capacity of the charging station n .
p^{DMax}	Capacity of the charging station at the depot.

C. Variables:

$C_{g,w}^{\text{DR}}$	DR cost of aggregator g .
$P_{b,w,t}, Q_{b,w,t}$	Active and reactive power in branch $b, b + 1$ at t and w .
$P_{b,w,t}^{\text{PV}}$	Power generation through PV panel b at t and w .
$P_{t,w}^{\text{APDN}}$	Power purchased from the market for the APDN at time t and scenario w without consideration of charging demands.

$P_{b,t,w}$	Overall power purchased from the market for the APDN at time t , scenario w , and node b including charging demands.
$P_{g,b,w,t}^{LC}$	Power curtailed by the aggregator g in APDN node b , at timeslot t and scenario w .
$P_{g,b,w,t}^{LS}$	Power shifted by aggregator g in APDN node b , at timeslot t and scenario w .
$Q_{b,t}^{CAP}$	Reactive power of capacitor banks at APDN node b , and time t .
$V_{b,w,t}$	Magnitude of voltage at APDN node b time t and scenario w .
$\Delta V_{b,w,t}$	Deviation of voltage from the minimum bound of APDN node b at t and w .
$\lambda_{g,t,w}^{AG}$	Offering price to DR aggregator g at t and w .
$P_{b,w,t}^{PV}$	PV generation at APDN node b , timeslot t and scenario w .
e_{inj}^{Ter}	En-route charging energy at terminal n between trips i and j .
e_{ij}^{Dep}	Received energy at the depots by the bus after trip i at depot $j \in D$.
SOC_{oi}	Energy of the bus when it leaves the depot before the first trip i .
SOC_{ij}	Energy level of the bus after trip i and exactly before starting trip j .
SOC_i	Amount of remaining energy in the battery upon finishing trip i .
$p_{inj,t}^{Ter}$	Power received by the bus at the stations (en-route) at t , after trip i and before trip j .
$p_{ij,t}^{Dep}$	Power received by the bus at the depot at t , after trip i at depot $j \in D$.
$C_{g,t,w}^{EQ}$	Auxiliary variable substituting with nonlinear bi-product.
x_{ij}	Binary variable defining the chain of trips.

D. Abbreviations:

APDN	Active power distribution network.
BEB	Battery electric bus.
DR	Demand response.
KKT	Karush–Kuhn–Tucker.
PDN	Power distribution network.
PV	Photovoltaic.

(Perumal et al., 2022; Dong et al., 2024). Furthermore, transport electrification intensifies the existing energy demands on power distribution networks (PDNs), potentially resulting in challenges in energy systems particularly during peak charging periods (Hartvigsson et al., 2022).

The existing literature extensively discusses studies on the charging scheduling of BEB and the application of Demand Response (DR) flexibility within power systems to support transport electrification. However, a significant gap exists in investigating the impact of BEB charging schedules on PDNs. Current efforts primarily focus on enhancing BEB transit systems or integrating flexibility into standalone Active Power Distribution Networks (APDN), characterized by controllable resources such as vehicle-to-grid (V2G) technology, energy storage systems, DR services, and distributed renewable energy sources. There is a notable scarcity of studies addressing approaches to mitigate the adverse effects of charging demand from BEB transit systems on PDNs through the utilization of flexible PDN resources. The current studies either limit the coupled operation of BEB transit systems to deploying BEBs solely for grid restoration purposes or neglect the broader impacts of BEBs on PDNs altogether. To address this gap, we propose an integrated framework involving BEB transit systems and APDN to analyze the implications of BEB charging demands on PDN operations. Moreover, we advocate for the integration of DR services to alleviate the adverse effects of BEB charging demands on APDN. Generally, two primary solutions exist for accommodating the additional charging demands of BEBs alongside existing APDN requirements: enhancing electricity generation capacity through new generator installations and managing demand-side flexibility to facilitate the integration of new charging demands within APDN constraints. Our emphasis in this study is on leveraging demand-side management flexibility to mitigate technical constraints, rather than relying solely on new generation installations to address the simultaneous electricity demands of existing infrastructure and newly introduced BEB charging requirements.

Motivated by these challenges, we propose a novel framework aimed at optimizing the charging operations of integrated BEB transit systems and APDN. The primary objective is to effectively support BEB mobility services by addressing their spatial and temporal charging demands. Special emphasis is placed on leveraging APDN capabilities to facilitate BEB operations with minimal costs, while ensuring compliance with power system constraints imposed by charging demands. In our envisioned framework, a non-profit third-party entity administers the integrated BEB-APDN system to optimize both BEB charging scheduling and APDN electricity procurement costs. The proposed approach employs a bi-level leader-follower Stackelberg game to model interactions among stakeholders, thereby minimizing the overall costs associated with the integrated BEB-APDN system. This research endeavors to foster sustainable development of BEBs in diverse urban settings characterized by power system constraints, and aims to enhance the efficiency of BEB operations through optimized charging scheduling and operational strategies.

The paper is structured as follows: Section 2 reviews the relevant work. Section 3 introduces the problem description and presents the mathematical modeling. Section 4 outlines the solution methodology. Section 5 presents the results of a case study. Lastly, Section 6 provides the concluding remarks.

2. Literature review

This section reviews the pertinent literature in three main areas: charging scheduling of BEBs, coupled optimization of transport and power distribution networks, and application of DR in APDNs.

The scheduling of BEBs for charging is a critical process that ensures sufficient energy is available for pre-scheduled service trips. Consequently, a significant body of research has concentrated on the challenges associated with charging scheduling, exploring various objectives. Charging scheduling of BEB transit systems and charging infrastructure planning were addressed in He et al. (2023), neglecting the impact of charging scheduling or infrastructure planning on the PDN. The charging scheduling problem concerning the battery degradation and constraints of charging facility capacities was proposed in Zhang and Yang (2024) using a partial charging strategy. The partial charging strategy gives the possibility to recharge with any amount of energy up to full capacity, deploying time-of-use prices. The uncertainty regarding energy consumption in charging accessibility through en-route charging was explored in Zeng et al. (2024). The uncertainty was addressed through a robust optimization approach, with charging energy performed under time-of-use electricity prices. Moreover, the possibility of deploying hybrid charging options including plugged-in and battery swapping in the scheduling of BEBs, was suggested in Huang et al. (2023) subject to the uncertainty of remaining capacity upon arrival at the station. Guschinsky et al. (2023) has concentrated on practical aspects of charging in a single depot problem, encompassing the non-linear nature of charging profile, various types of chargers and batteries, cyclic wear of batteries, various charging strategies such as partial charging strategy, interruption in the charging process, using switching to avoid interruption, and minimizing total number of switching. In Li et al. (2024) and Zhong et al. (2024), the charging scheduling was investigated while BEBs were charged in motion using wireless lanes. To achieve this, a bi-level framework was proposed, incorporating the planning of charging lanes at the upper level and the charging scheduling problem at the lower level. In Wang et al. (2023), the conflict of charging during the dwelling of passengers was presented alongside an emphasis on battery degradation in the deployment of fast chargers for charging scheduling of BEBs. A charging scheduling problem was implemented in Bao et al. (2023), operating across multiple bus lines and multiple depots and terminals, towards determining an optimal solution for the location and time of charging given a pre-scheduled timetable. In Xie et al. (2023), three aspects were considered simultaneously: scheduling of charging, buses, and drivers by deploying a collaborative scheme incorporating multiple charging modes. Moreover, the ramifications of multiple depots and partial charging policy in charging scheduling were explored in Zhou et al. (2024a). The partial charging policy offers flexibility to charging time due to a short dwell time for full replenishment, particularly during peak hours when bus schedules are tightly packed. Cui et al. (2023) suggested a joint framework to address the optimization of the vehicle and recharging scheduling under the limitation of a number of chargers to serve trips adhered to a pre-established bus timetable. Despite a number of relevant studies about charging optimization of BEB, current methodologies predominantly adopt a standalone optimization of charging scheduling and neglect the impacts of charging demand on PDNs and constraints from PDN on the charging optimization of BEB. Several studies have concentrated on the detailed aspects of scheduling battery electric buses (BEBs). For example, Zhou et al. (2024a) investigated the heterogeneity of BEBs in scheduling, while Avishan et al. (2023) addressed the BEB scheduling and procurement problem, incorporating uncertainties related to energy consumption and travel time.

In recent years, researchers have shown interest in exploring various aspects of coupled transport systems and power distribution networks. However, the majority of studies have predominantly explored coupled systems for private electric vehicles. For instance, Qiao et al. (2022), Li et al. (2023) and Shao et al. (2023) delved into the behavior of selfish drivers leading to road congestion in their pursuit of charging stations. The coupling of PDNs and BEB transit systems has also been investigated in several studies. Shaheen et al. (2021) and Ren et al. (2022) presented a framework to highlight the benefits of integrating the set of photovoltaics (PVs) and battery electric storage in PDNs. The former investigated the impact of a set of PVs and batteries in the reduction of total operation costs and emissions. The latter focused on the payback period of implementing PV and battery in the BEB transit system. The impact of fast charging stations on PDN demands was explored in Lin et al. (2019), which disregarded the charging scheduling of BEBs by concentrating on large-scale planning of charging stations. Additionally, El-Taweel et al. (2020) investigated how energy consumption affects the adoption of BEBs. Then, the given approach considered the operational requirements of BEB transit systems to integrate with a PDN in order to develop a PDN-BEB formulation for the optimal design of BEB transit systems. Similarly, Mohamed et al. (2017) examined the impact of various charging strategies for BEBs, such as overnight and fast charging, on PDNs. This research included the design of the necessary infrastructure for charging stations. Some studies have also suggested the utilization of BEBs in facing hazardous cases in PDNs. Wu et al. (2023) proposed the integration of BEBs to restore PDNs. Restoration in PDNs involves the process of restoring electrical power to customers following an outage or disruption. Although the electrical part was addressed comprehensively, BEB scheduling was carried out to fulfill the objectives of the PDN operator. Similarly, the deployment of idle BEBs to restore the PDN was studied by Li et al. (2021). Nevertheless, these studies have not primarily addressed the impact of BEB transit systems on the technical constraints of PDNs, such as voltage drop or branch overload.

Exploring the management of APDN in the presence of flexibility resources has been a focal point in the power systems. The application of DR in coordination with neighboring APDN was investigated in Homaee et al. (2023) wherein the DR flexibility was modeled when the APDN were situated in different areas of pricing in an electricity market. The coordination of electrified road systems with APDN was proposed in Najafi et al. (2024) to investigate the traffic assignment problem and its impact on APDN. A time

Table 1

Overview of the literature review and the including items in their approach.

Reference	Transportation mode	Charging scheduling	Coupled systems	APDN flexibility	RES	Uncertainty
He et al. (2023), Guschinsky et al. (2023), Li et al. (2024), Wang et al. (2023), Bao et al. (2023), Zhou et al. (2024a), Cui et al. (2023) and Zhang and Yang (2024)	BEB	✓	✗	✗	✗	✗
Zeng et al. (2024) and Huang et al. (2023)	BEB	✓	✗	✗	✗	✓
Qiao et al. (2022), Li et al. (2023) and Shao et al. (2023)	Private car	✓	✓	✗	✗	✗
Shaheen et al. (2021) and Ren et al. (2022)	Private car	✓	✓	✗	✓	✓
Najafi et al. (2024)	Private car	✗	✓	✓	✓	✓
Lin et al. (2019)	BEB	✗	✓	✗	✗	✗
El-Taweel et al. (2020) and Mohamed et al. (2017)	BEB	✓	✓	✗	✗	✗
Li et al. (2021)	BEB	✓	✓	✗	✗	✗
Wu et al. (2023)	BEB	✓	✓	✗	✓	✓
Proposed method	BEB	✓	✓	✓	✓	✓

of use DR was presented in [Bahawan et al. \(2022\)](#) as a means to optimally manage a power distribution network, addressing other energy carriers and electric vehicle charging. The effect of main flexibility resources encompassing DR, V2G, and battery electric storage was studied in [Sivasankari and Narayanan \(2022\)](#). The deployment of DR, alongside other flexibility resources such as V2G and battery storage, was found to enhance APDN revenue and provide a broader and more reliable supply to consumers. In [Wen et al. \(2024\)](#), a dynamic price-based DR model was explored, utilizing clustering and game theory concurrently to enable consumers to reduce peak consumption while maximizing the utility of electricity service providers. The type of consumer was determined through clustering, and the interaction between the consumer and the DR provider was modeled via game theory principles. However, there is no research addressing the coupled BEB-APDN optimization leveraging DR, to our best knowledge.

For better understanding of existing research, [Table 1](#) provides a comparative analysis of the topics addressed in each cited study. It is important to clarify that the terms “coupled system” and “APDN flexibility” refer to whether the studies incorporate the BEB-APDN framework and DR flexibility, respectively. The column labeled ‘uncertainty’ indicates whether the references consider any form of uncertainty, utilizing stochastic methods to address these complexities in the proposed solutions. Additionally, the application of renewable energy sources (RES) is specified in a separate column.

3. Modeling framework

3.1. Problem description

We take into account a coupled system comprising the BEB transit system and APDN scheduled within a time horizon \mathcal{T} . The joint problem aims at minimizing total expected cost ($\mathbb{E}[C]$) for operating BEB constrained by the APDN, which encompasses the cost of bus fleets to satisfy timetables of BEB transit system C^{BEB} and total cost of electricity procurement from APDN (C_w^{APDN}) over a set \mathcal{W} of scenarios, as in

$$\mathbb{E}[C] = \sum_{w \in \mathcal{W}} \rho_w \cdot (C_w^{\text{BEB}} + C_w^{\text{APDN}}). \quad (1)$$

The total cost of electricity procurement from APDN consist of electricity for charging BEB and the electricity demand of other sectors such as residential usage demand. The APDN interacts with DR aggregators ($g \in \mathcal{G}$) that seek to maximize their own profit. The concept of DR flexibility is predicated on the premise that, in the absence of DR, the cumulative charging demand from BEBs, combined with the demand from other sectors, may exceed the technical constraints of the APDN, especially in peak hours. DR can alleviate the electricity demand burden from these other sectors, thereby enabling the APDN to adequately support the charging requirements of BEBs. This strategic modulation of demand ensures that the APDN operational limits are not breached, enhancing the overall efficiency and reliability of BEB system. The DR aggregators are active entities at the lower level that interact with the coupled BEB-APDN system at the upper level. It is assumed that there is a non-profit governmental entity that oversees the operations of both BEB and APDN systems. The non-profit entity can procure electricity from a day ahead electricity market from the upstream to support charging demands and the existing demands on the APDN. Both electricity prices and PV generations are subject to uncertainty. [Fig. 1](#) depicts the schematic of the coupled systems interacting with DR aggregators. Please note that the definitions and meanings of all variables in this section are summarized in nomenclature section at the beginning of this paper to reduce redundancy.

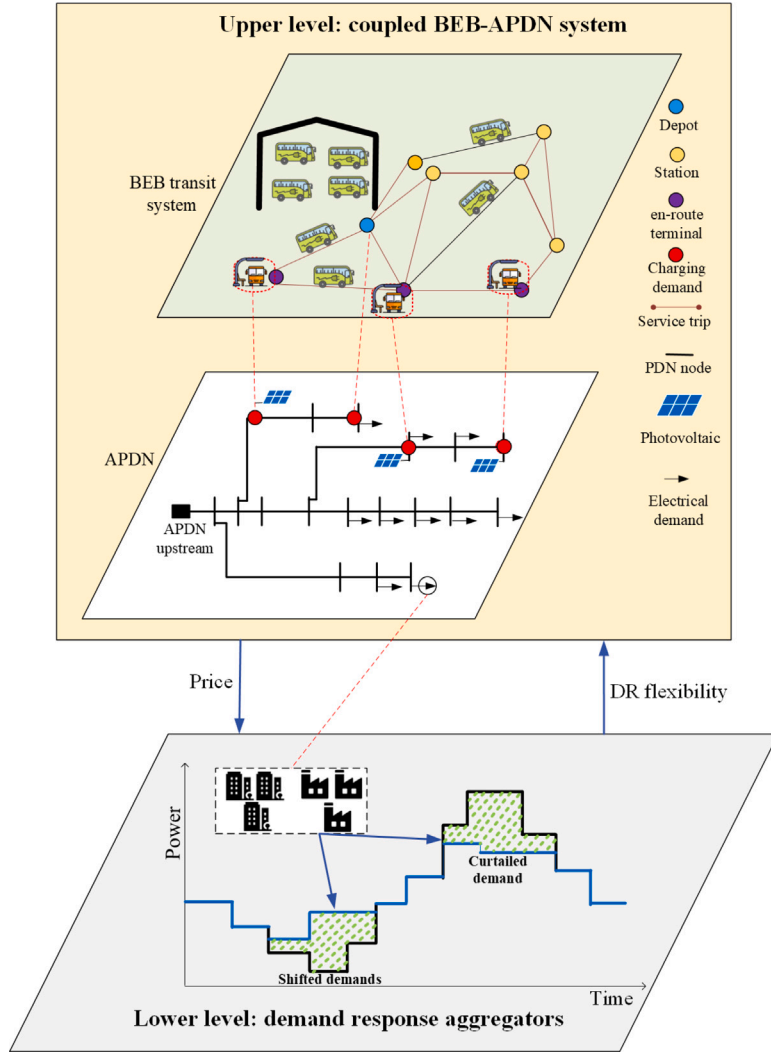


Fig. 1. Schematic of the coupled BEB-APDN system interacting with demand response aggregators.

We define overlapped sets to present our approach. Let $I = \mathcal{O} \cup S \cup D$ denote the set comprising all trips in the timetables of BEB, encompassing the first trip from the origin bus depot (\mathcal{O}), all trips excluding the first and last trips (S), and the last trip to destination depot (D) after a day. We define two additional sets to include the first trip with all service trips as $\mathcal{OS} = \mathcal{O} \cup S$ and the last trip with all service trips $SD = D \cup S$. The BEB transit system and the APDN are defined over sets of \mathcal{N} and \mathcal{B} , respectively. Certain nodes (i.e. charging stations) within the BEB transit system denoted by the set $\mathcal{N}^B \subset \mathcal{N}$ are connected to the APDN through the nodes of APDN specified as $\mathcal{B}^N \subset \mathcal{B}$. Meanwhile, some nodes of APDN are virtually connected with and managed by DR aggregators specified as $\mathcal{B}^G \subset \mathcal{B}$.

The coupling between BEB and APDN systems arises from the charging demand from BEBs ($P_{b,w,t}^{BEB}$), which is fed through charging stations connected to the APDN. It is worth mentioning that the APDN is the only source to support charging demands in our study. The set of variables of BEB transit system and APDN are denoted as $\mathcal{V}_{w,t}^{BEB}$ and $\mathcal{V}_{w,t}^{APDN}$, respectively. The set of feasible operational solutions are defined as \mathcal{F}^{BEB} and \mathcal{F}^{APDN} , respectively. Therefore, our upper-level objective manifests as the following cost-minimization problem.

$$\begin{aligned} \min \quad & \left\{ \sum_{w \in \mathcal{W}} \rho_w \cdot (C_w^{BEB} + C_w^{APDN}) \right\} \\ \text{over} \quad & \left(\mathcal{V}_{w,t}^{BEB} \cup \mathcal{V}_{w,t}^{APDN} \right)_{w \in \mathcal{W}, t \in \mathcal{T}} \end{aligned} \quad (2)$$

subject to

$$\mathcal{V}_{w,t}^{BEB} \in \mathcal{F}^{BEB}, \quad \forall t \in \mathcal{T}, \quad (3)$$

$$\gamma_{w,t}^{\text{APDN}} \in \mathcal{F}^{\text{APDN}}, \quad \forall t \in \mathcal{T}, \quad (4)$$

$$P_{b,w,t}^{\text{BEB}}, \quad \forall b \in \mathcal{B}^{\text{N}}, w \in \mathcal{W}, t \in \mathcal{T}. \quad (5)$$

In the following sub-section, we present the details of objective functions, decision variables, and constraints in optimizations of each system.

3.2. BEB transit system

The operational and charging scheduling of BEB transit systems must adhere to pre-designed timetables, encompassing all service trips. Each bus may serve some trips on various routes, while one trip is performed only by one bus. To apply the operational scheduling of BEBs, we define a binary variable x_{ij} , indicating the connection of trips. If trip i is connected to trip j , x_{ij} is one; otherwise, it is zero (Duan et al., 2023). The objective function in operational and charging scheduling is to deploy the minimum number of BEBs to serve trips and use the minimum cost to support charging demands.

$$\min C^{\text{BEB}} = \sum_{i \in \mathcal{S}} \sum_{o \in \mathcal{O}} \lambda^{\text{BEB}} x_{oi} + \sum_{i \in \mathcal{T}} \sum_{b \in \mathcal{B}^{\text{N}}} \sum_{w \in \mathcal{W}} \rho_w \lambda_{t,w}^{\text{M}} P_{b,w,t}^{\text{BEB}}. \quad (6)$$

The scheduling of BEBs is subject to three constraints. Eq. (7) indicates that each tip is served only once. The conservation flow constraint, defining the equality of inflow and outflow of bus trips in a terminal, is given in (8) (Li et al., 2021). Eq. (9) ensures that trip j is performed after trip i without any overlap in time, considering the deadhead trip time.

$$\sum_{j \in \mathcal{S}, i \neq j} x_{ij} = 1, \quad \forall i \in \mathcal{S}, \quad (7)$$

$$\sum_{i \in \mathcal{S}, i \neq j} x_{ji} - \sum_{i \in \mathcal{O}, i \neq j} x_{ij} = 0, \quad \forall j \in \mathcal{S}, \quad (8)$$

$$\bar{u}_i + \tau_i + \tau_i^{\text{DH}} \leq \underline{u}_j + M(1 - x_{ij}), \quad \forall i, j \in \mathcal{S}, i \neq j. \quad (9)$$

Upon departure from the depot, each bus initiates its first trip fully (or near fully) charged. Subsequently, each bus performs the trips and replenishes its energy solely en route between trips. En-route charging refers to the process of recharging BEBs at bus stops along a route where sufficient time is available for the charging operation. While the proposed optimization methodology accommodates the possibility of charging at any bus stop, the present case study is limited to charging activities conducted exclusively at the starting or ending bus stops, stations, or depots upon trip completion. This focus is justified by the short stopping durations at intermediate bus stops, which in this study are typically limited to 1–2 min. The BEBs do not return to the depot until completing the entire chain of trips in a day. It means that each bus returns to the depot upon finishing its last trip in a day, typically in the evening. The BEB transit system model should ensure the level of energy satisfy the energy consumption of all trips during the chain of trips, including in the depot, first trip, last trip, and other daily trips. Hence, we represent the matter mathematically as follows. Based on the assumption, the BEBs leave the depot nearly fully charged (here, over 90% of the capacity). Therefore, Eq. (10) reflects this aspect.

$$SOC_{oi} = x_{oi} \bar{Y}A, \quad \forall i \in \mathcal{S}, o \in \mathcal{O}. \quad (10)$$

The energy level should also adhere to its restrictions throughout the daily trips. We define the variable $S\bar{O}C_i$ to denote the energy level in the battery of BEB after completing trip i . The remaining energy after finishing trip i is updated based on the energy consumed during the trips (c_i^{SL}) and also from the depot to the first trip (SOC_{oi}), as specified in (11). Additionally, there is the possibility of recharging BEBs between the trips. It should be noted that a BEB cannot return to the depot before finishing all its daily trip. Hence, the BEB can only recharge en route after leaving the depot. Eq. (12) illustrates the amount of battery energy after finishing trip i and before trip j . It is important to note the potential for recharging the battery between consecutive trips en route. Upon completing all service trips of a day, the bus returns to the depot. It is crucial to ensure sufficient energy for the deadhead trip from the last service trip to the depot. Eq. (13) indicates the energy in batteries required for a deadhead trip to the depot after the last trip. It is worth mentioning that the three mentioned constraints are valid when there is a connection between the trips ($x_{ij} = 1$); otherwise, the equations are changed to self-evident constraints (He et al., 2023).

$$S\bar{O}C_i \leq (SOC_{oi} - c_{oi}^{\text{O2S}} - c_i^{\text{SL}})x_{oi} + \bar{Y}A(1 - x_{oi}), \quad \forall i \in \mathcal{S}, o \in \mathcal{O}, \quad (11)$$

$$S\bar{O}C_j \leq (S\bar{O}C_i + e_{inj}^{\text{Ter}} - c_{ij}^{\text{ST}} - c_j^{\text{SL}})x_{ij} + \bar{Y}A(1 - x_{ij}), \quad \forall i, j \in \mathcal{S}, i \neq j, \quad (12)$$

$$SOC_{ij} \leq (S\bar{O}C_i - c_{ij}^{\text{S2D}})x_{ij} + \bar{Y}A(1 - x_{ij}), \quad \forall i \in \mathcal{S}, j \in \mathcal{D}. \quad (13)$$

In any situation during daily trips, the energy of the BEBs should adhere to its capacity range. The updated energy value in (11) compiles with the energy range specified in (14). The energy level during the trips and after recharging Eq. (15) and energy consumption for the next deadhead trip for the next service trip j in Eq. (16) are bounded by the upper and lower limits of battery capacity. Additionally, the remaining energy after the last trip to the depot conforms to the battery capacity bound specified in (17).

$$\underline{Y}Ax_{oi} \leq (SOC_{oi} - c_{oi}^{O2S} - c_i^{SL})x_{oi} \leq \bar{Y}Ax_{oi}, \quad \forall i \in S, o \in \mathcal{O}, \quad (14)$$

$$\underline{Y}Ax_{ij} \leq (S\bar{O}C_i + e_{inj}^{Ter})x_{ij} \leq \bar{Y}Ax_{ij}, \quad \forall i, j \in S, \quad (15)$$

$$\underline{Y}Ax_{ij} \leq (S\bar{O}C_i + e_{inj}^{Ter} - c_{ij}^{ST} - c_j^{SL})x_{ij} \leq \bar{Y}Ax_{ij}, \quad \forall i, j \in S, \quad (16)$$

$$\underline{Y}Ax_{ij} \leq (S\bar{O}C_i - c_{ij}^{S2D})x_{ij} \leq \bar{Y}Ax_{ij}, \quad \forall i \in S, j \in D. \quad (17)$$

The following constraints delineate the level of energy in the depot. The BEB is expected to undergo recharging at the depot upon finishing all service trips to a predetermined energy level to prepare for service trips of the next day (18). Meanwhile, the energy of BEBs in the depot respects its upper and lower restrictions in (19).

$$(SOC_{ij} + e_{ij}^{Dep})x_{ij} \geq \bar{Y}Ax_{ij}, \quad \forall i \in S, j \in D, \quad (18)$$

$$\underline{Y}Ax_{ij} \leq SOC_{ij}x_{ij} \leq \bar{Y}Ax_{ij}, \quad \forall i \in S, j \in D. \quad (19)$$

The energy of BEBs received from chargers en route and in the depot is indicated in Eqs. (20) and (21), respectively.

$$e_{inj}^{Ter} = \frac{1}{|\mathcal{T}|} \sum_{t \in \mathcal{T}} p_{injt}^{Ter}, \quad \forall i, j \in S, n \in \mathcal{N}^B, \quad (20)$$

$$e_{ij}^{Dep} = \frac{1}{|\mathcal{T}|} \sum_{t \in \mathcal{T}} p_{ijt}^{Dep}, \quad \forall i \in S, j \in D. \quad (21)$$

The charging received from the APDN is limited through the charging station capacity in both charging option of en route and in depot, as in

$$p_{injt}^{Ter} \leq x_{ij} p_n^{EnMax}, \quad \forall i, j \in S, i \neq j, t \in [\bar{u}_i + \tau_i^{DH}, \underline{u}_j - \tau_j^{DH}], n \in \mathcal{N}^B, \quad (22)$$

$$p_{ijt}^{Dep} \leq x_{ij} p^{DMax}, \quad \forall i \in S, j \in D, i \neq j, t \in \{[\underline{u}_i - \tau_i^{O2S}] \cup [\bar{u}_j + \tau_j^{S2D}]\}. \quad (23)$$

3.3. APDN model

The APDN aims to minimize its total cost of electricity procurement from BEBs and other sectors through engagement with the wholesale electricity market and DR aggregators. The objective function of the APDN is given as

$$C_w^{APDN} = \sum_{t \in \mathcal{T}} P_{t,w}^{APDN} \lambda_{w,t}^M + C_w^{DR}, \quad \forall w \in \mathcal{W}, \quad (24)$$

where C_w^{APDN} is the total cost of APDN including procuring electricity and interactions with DR aggregators. C_w^{DR} represents the operational cost of DR aggregators. We formulate a radial APDN wherein node $b \in \mathcal{B}$ and $b+1 \in \mathcal{B}$ are exclusive sequent nodes. The active and reactive power balance for each node is defined by the power flow model (Wang et al., 2016; Baran and Wu, 1989).

$$P_{b+1,w,t} = P_{b,w,t} - r_b I_{b,w,t} - p_{b,w,t}, \quad \forall b \in \mathcal{B}, w \in \mathcal{W}, t \in \mathcal{T}, \quad (25)$$

and

$$Q_{b+1,w,t} = Q_{b,w,t} - x_b I_{b,w,t} - q_{b,w,t}, \quad \forall b \in \mathcal{B}, w \in \mathcal{W}, t \in \mathcal{T}, \quad (26)$$

where $P_{b,w,t}$ and $Q_{b,w,t}$ represent the active and reactive power flowing between nodes b and $b+1$, respectively. $I_{b,w,t}$ denotes the squared magnitude of the current of the line. The resistance and reactance of the lines are denoted by r_b and x_b , respectively. $p_{b,w,t}$ and $q_{b,w,t}$ indicate the node net active and reactive power injection. The net power injections are represented in the following equations using the flexibility of DR and generations of PVs.

$$P_{b,w,t} = D_{b,t}^P + \sum_{g \in \mathcal{G}} (P_{g,b,w,t}^{LS} - P_{g,b,w,t}^{LC}) - P_{b,w,t}^{PV} + P_{b,w,t}^{BEB}, \quad \forall b \in \mathcal{B}, w \in \mathcal{W}, t \in \mathcal{T}, \quad (27)$$

where $P_{b,w,t}^{PV}$ represents the generation of PV, $D_{b,t}^P$ denotes power demand, $P_{g,b,w,t}^{LC}$ is load curtailment, and $P_{g,b,w,t}^{LS}$ indicates load shifting. The effect of charging demands is denoted by $P_{b,w,t}^{BEB}$ and $P_{t,w}^{APDN} = p_{b,w,t} - P_{b,w,t}^{BEB}$.

The reactive power injection is represented similarly as

$$q_{b,w,t} = D_{b,t}^Q - Q_{b,t}^{CAP}, \quad \forall b \in \mathcal{B}, w \in \mathcal{W}, t \in \mathcal{T}, \quad (28)$$

where $Q_{b,t}^{\text{CAP}}$ indicates the reactive power injection of the node capacitor bank. The voltage drop between $b + 1$ and b is measured by

$$V_{b,w,t} - 2(r_b P_{b,w,t} + x_b Q_{b,w,t}) - (r_b^2 + x_b^2) I_{b,w,t} = V_{b+1,w,t}, \quad \forall b \in \mathcal{B}, w \in \mathcal{W}, t \in \mathcal{T}, \quad (29)$$

where $V_{b,w,t}$ is the squared magnitude of the APDN node's voltage. Branch power flows are obtained using the second-order conic relaxation model inequality as presented in Low (2014).

$$V_{b,w,t} I_{b,w,t} \geq P_{b,w,t}^2 + Q_{b,w,t}^2, \quad \forall b \in \mathcal{B}, s \in \mathcal{W}, t \in \mathcal{T}. \quad (30)$$

The voltage magnitude should adhere to the safe bounds as

$$\underline{V} \leq V_{b,w,t} \leq \bar{V}, \quad \forall b \in \mathcal{B}, w \in \mathcal{W}, t \in \mathcal{T}. \quad (31)$$

A PV generation should also meet its upper and lower bounds, as in

$$0 \leq P_{b,w,t}^{\text{PV}} \leq \bar{P}_{b,w,t}^{\text{PV}}, \quad \forall b \in \mathcal{B}, w \in \mathcal{W}, t \in \mathcal{T}, \quad (32)$$

where the (maximum) PV generation $\bar{P}_{b,w,t}^{\text{PV}}$ is a scenario-dependent parameter.

3.4. Demand response flexibility

A flexible electricity demand can be adjusted in response to signals from the operator of the APDN. The adjustment refers to curtailment or (and) shifting part of loads to other hours based on the preferences of consumers. Since individual consumers are not large enough, an aggregator is assigned to collect the flexibility and interact with the operator. Indeed, the aggregator acts on behalf of the consumer and decides whether to shift or curtail based on the received price signal from the APDN operator. For ease of presentation, we assume one load at each APDN node. The amount of flexibility of demands is obtained in response to the DR prices $\lambda_{g,t,w}^{\text{AG}}$. Each aggregator engages in the co-optimization of a portfolio comprising flexible loads, by determining the amount of energy that can be shifted or curtailed, with the purpose of either minimizing its energy cost or maximizing its profit. It is formulated through the optimization problem, as in

$$C_{g,w}^{\text{DR}} = \min_{\Xi} \left\{ \sum_{t \in \mathcal{T}} \sum_{b \in \mathcal{B}} \mathbb{I}_{bg} \left(P_{g,b,w,t}^{\text{LC}} \cdot (c_{b,t}^{\text{DR}} - \lambda_{g,t,w}^{\text{AG}}) + \lambda_b^{\text{NS}} P_{g,b,w,t}^{\text{NS}} \right) \right\}, \quad \forall w \in \mathcal{W}, g \in \mathcal{G}, \quad (33)$$

where \mathbb{I}_{bg} indicate whether the load at APDN node b is registered with the aggregator $g \in \mathcal{G}$. Ξ denotes the set of decision variables at the lower-level problem, which represents the DR program decision variables, including $P_{g,b,w,t}^{\text{LC}}$, $P_{g,b,w,t}^{\text{LS}}$, $P_{g,b,w,t}^{\text{NS}}$, $c_{b,t}^{\text{DR}}$, and λ_b^{NS} signify the cost parameters representing the compensation that the aggregator pays to the load users when curtailing or not serving, respectively. The total cost at the lower level in each scenario is obtained as

$$C_w^{\text{DR}} = \sum_{g \in \mathcal{G}} C_{g,w}^{\text{DR}}, \quad \forall w \in \mathcal{W}. \quad (34)$$

The proposed objective functions are subject to the constraints of the DR program. Here, we present the constraints, where the dual variable of each constraint is given after the colon. The aggregator is not allowed to shift the energy more than those curtailed. This matter is represented mathematically, as in

$$\sum_{t \in \mathcal{T}} P_{g,b,w,t}^{\text{LS}} \leq \sum_{t \in \mathcal{T}} P_{g,b,w,t}^{\text{LC}}, \quad : \phi_{g,b,w}, \quad \forall b \in \mathcal{B}, w \in \mathcal{W}, g \in \mathcal{G}. \quad (35)$$

Any shortage in the shift of curtailed energy is interpreted as no supplied energy, which has to be compensated as mentioned in the last term of (33). The not-supplied energy is obtained as in,

$$P_{g,b,w,t}^{\text{NS}} = \sum_{t \in \mathcal{T}} P_{g,b,w,t}^{\text{LC}} - \sum_{t \in \mathcal{T}} P_{g,b,w,t}^{\text{LS}}, \quad : \delta_{g,b,w}, \quad \forall b \in \mathcal{B}, w \in \mathcal{W}, g \in \mathcal{G}. \quad (36)$$

The total curtailment and shift cannot exceed a certain portion of the demands over the period and in each time-slot, as in

$$\sum_{t \in \mathcal{T}} P_{g,b,w,t}^{\text{LS}} \leq \sum_{t \in \mathcal{T}} \Lambda_b D_{b,t}^{\text{P}}, \quad : \omega_{g,b,w}, \quad \forall b \in \mathcal{B}, w \in \mathcal{W}, g \in \mathcal{G}, \quad (37)$$

$$\sum_{t \in \mathcal{T}} P_{g,b,w,t}^{\text{LC}} \leq \sum_{t \in \mathcal{T}} \Lambda_b D_{b,t}^{\text{P}}, \quad : \sigma_{g,b,w}, \quad \forall b \in \mathcal{B}, w \in \mathcal{W}, g \in \mathcal{G}, \quad (38)$$

$$P_{g,b,w,t}^{\text{LS}} \leq \Phi_b D_{b,t}^{\text{P}}, \quad : \alpha_{g,b,w,t}, \quad \forall t \in \mathcal{T}, b \in \mathcal{B}, w \in \mathcal{W}, g \in \mathcal{G}, \quad (39)$$

$$P_{g,b,w,t}^{\text{LC}} \leq \Phi_b D_{b,t}^{\text{P}}, \quad : \varpi_{g,b,w,t}, \quad \forall t \in \mathcal{T}, b \in \mathcal{B}, w \in \mathcal{W}, g \in \mathcal{G}. \quad (40)$$

4. Solution algorithms

The proposed framework takes into account the coupled BEB-APDN system at the upper-level and the set of DR aggregators at the lower-level. The relation of the BEB-APDN and DR aggregators constitutes a leader-follower Stackelberg game. Hence, the lower-level problem is transferred to the upper-level using Karush–Kuhn–Tucker (KKT) conditions (Yi et al., 2021; Zhao et al., 2021). In this section, we provide the methodology for transferring the bi-level model to the equivalent single model using KKT conditions. The deployed linearization methods are presented as well.

4.1. BEB-APDN upper-level problem

At the upper level, the non-profit entity manages both the BEB transit system and APDN. Hence, both objectives are integrated into the upper-level problem. The objective function in (41) represents the coupled objective. Notably, the last term accounts for the cost of interaction with the set of DR aggregators at the lower-level.

$$\min \sum_{t \in \mathcal{T}} \sum_{w \in \mathcal{W}} \sum_{b \in \mathcal{B}} \rho_w \left(\sum_{o \in \mathcal{O}} \lambda^{\text{BEB}} x_{oi} + \lambda_{t,w}^{\text{M}} p_{b,w,t} + \sum_{g \in \mathcal{G}} \lambda_{g,t,w}^{\text{AG}} P_{g,b,w,t}^{\text{LC}} \right). \quad (41)$$

4.2. Demand response aggregator lower-level problem

The set of DR aggregators establishes the lower-level problem. We utilize the well-known KKT condition to bring the lower-level constraints to the upper level and construct a single-level model (Carrion et al., 2009). Eqs. (42) to (49) indicate the derived equations.

$$c_{b,t}^{\text{DR}} - \delta_{g,b,w} + \sigma_{g,b,w} + \varpi_{g,b,w,t} - \phi_{g,b,w} - \lambda_{g,t,w}^{\text{AG}} = 0, \quad (42)$$

$$\delta_{g,b,w} + c_b^{\text{LL}} = 0, \quad (43)$$

$$\phi_{g,b,w} + \delta_{g,b,w} + \omega_{g,b,w} + \alpha_{g,b,w,t} = 0, \quad (44)$$

$$\omega_{g,b,w} \left(\sum_{t \in \mathcal{T}} P_{g,b,w,t}^{\text{LS}} - \sum_{t \in \mathcal{T}} \Lambda_b D_{b,t}^{\text{P}} \right) = 0, \quad \forall g \in \mathcal{G}, b \in \mathcal{B}^{\text{G}}, w \in \mathcal{W}, \quad (45)$$

$$\sigma_{g,b,w} \left(\sum_{t \in \mathcal{T}} P_{g,b,w,t}^{\text{LC}} - \sum_{t \in \mathcal{T}} \Lambda_b D_{b,t}^{\text{P}} \right) = 0, \quad \forall g \in \mathcal{G}, b \in \mathcal{B}^{\text{G}}, w \in \mathcal{W}, \quad (46)$$

$$\phi_{g,b,w} \left(\sum_{t \in \mathcal{T}^{\text{D}}} P_{g,b,w,t}^{\text{LS}} - \sum_{t \in \mathcal{T}^{\text{I}}} P_{g,b,w,t}^{\text{LC}} \right) = 0, \quad \forall g \in \mathcal{G}, b \in \mathcal{B}^{\text{G}}, w \in \mathcal{W}, \quad (47)$$

$$\alpha_{g,b,w,t} (P_{g,b,w,t}^{\text{LS}} - \Phi_b D_{b,t}^{\text{P}}) = 0, \quad \forall g \in \mathcal{G}, b \in \mathcal{B}^{\text{G}}, w \in \mathcal{W}, \quad (48)$$

$$\varpi_{g,b,w,t} (P_{g,b,w,t}^{\text{LC}} - \Phi_b D_{b,t}^{\text{P}}) = 0, \quad \forall g \in \mathcal{G}, b \in \mathcal{B}^{\text{G}}, w \in \mathcal{W}. \quad (49)$$

In the given constraints, $\omega_{g,b,w}$, $\sigma_{g,b,w}$, $\phi_{g,b,w}$, $\varpi_{g,b,w,t}$ and $\alpha_{g,b,w,t}$ are non-negative dual variables.

4.3. Linearization techniques

The constraints derived in (45)–(49), known as complementary slackness conditions, consist of non-linear terms. We employ the big-M method to linearize them (Najafi et al., 2022), as in

$$\omega_{g,b,w} \leq M_1 U_{g,b,w}, \quad \forall g \in \mathcal{G}, b \in \mathcal{B}^{\text{G}}, w \in \mathcal{W}, \quad (50)$$

$$\sum_{t \in \mathcal{T}} P_{g,b,w,t}^{\text{LS}} - \sum_{t \in \mathcal{T}} \Lambda_b D_{b,t}^{\text{P}} \leq M_2 (1 - U_{g,b,w}), \quad \forall g \in \mathcal{G}, b \in \mathcal{B}^{\text{G}}, w \in \mathcal{W}, \quad (51)$$

$$\sigma_{g,b,w} \leq M_1 K_{g,b,w}, \quad \forall g \in \mathcal{G}, b \in \mathcal{B}^{\text{G}}, w \in \mathcal{W}, \quad (52)$$

$$\sum_{t \in \mathcal{T}} P_{g,b,w,t}^{\text{LC}} - \sum_{t \in \mathcal{T}} \Lambda_b D_{b,t}^{\text{P}} \leq M_2 (1 - K_{g,b,w}), \quad \forall g \in \mathcal{G}, b \in \mathcal{B}^{\text{G}}, w \in \mathcal{W}, \quad (53)$$

$$\phi_{g,b,w} \leq M_1 H_{g,b,w}, \quad \forall g \in \mathcal{G}, b \in \mathcal{B}^{\text{G}}, \quad (54)$$

$$\sum_{t \in \mathcal{T}^{\text{D}}} P_{g,b,w,t}^{\text{LS}} - \sum_{t \in \mathcal{T}^{\text{I}}} P_{g,b,w,t}^{\text{LC}} \leq M_2 (1 - H_{g,b,w}), \quad \forall g \in \mathcal{G}, b \in \mathcal{B}^{\text{G}}, w \in \mathcal{W}, \quad (55)$$

$$\alpha_{g,b,w,t} \leq M_1 R_{g,b,w,t}, \quad \forall t \in \mathcal{T}, g \in \mathcal{G}, b \in \mathcal{B}^{\text{G}}, w \in \mathcal{W}, \quad (56)$$

$$P_{g,b,w,t}^{LS} - \Phi_b D_{b,t}^P \leq M_2(1 - R_{g,b,w,t}), \quad \forall t \in \mathcal{T}, g \in \mathcal{G}, b \in \mathcal{B}^G, w \in \mathcal{W}, \quad (57)$$

$$\varpi_{g,b,w,t} \leq M_1 Y_{g,b,w,t}, \quad \forall t \in \mathcal{T}, g \in \mathcal{G}, b \in \mathcal{B}^G, w \in \mathcal{W}, \quad (58)$$

$$P_{g,b,w,t}^{LC} - \Phi_b D_{b,t}^P \leq M_2(1 - Y_{g,b,w,t}), \quad \forall t \in \mathcal{T}, g \in \mathcal{G}, b \in \mathcal{B}^G, w \in \mathcal{W}. \quad (59)$$

where $U_{g,b,w}$, $K_{g,b,w}$, $R_{g,b,w,t}$, $Y_{g,b,w,t}$, and $H_{g,b,w}$ are binary variables. The bilinear product $\lambda_{g,t,w}^{AG} P_{g,b,w,t}^{LC}$ in (33) is also a non-linear term. We use the strong duality theorem to linearize the product (Najafi et al., 2023), as in

$$C_{g,t,w}^{EQ} = - \sum_{b \in \mathcal{B}^G} \left(\sigma_{g,b,w} \Lambda_b D_{b,t}^P + \omega_{g,b,w} \Lambda_b D_{b,t}^P + \alpha_{g,b,w,t} \Phi_b D_{b,t}^P + \varpi_{g,b,w,t} \Phi_b D_{b,t}^P \right) + c_{b,t}^{DR} P_{g,b,w,t}^{LC} + \lambda_b^{NS} P_{g,b,w}^{NS}, \quad \forall g \in \mathcal{G}, w \in \mathcal{W}, t \in \mathcal{T}. \quad (60)$$

The trip chain binary variable representing the trip chain, denoted by x_{ij} is multiplied by (10)–(19), rendering them non-linear equations. The bus scheduling problem is conducted based on a predetermined timetable. Given that the constraints governing bus scheduling (Eqs. (7)–(9)) are entirely distinct from those governing charging scheduling, we can simply separate the problem into two distinct ones. In the first step of the problem, the bus schedule is solved, as in

$$\min C^{BEB} = \min \sum_{i \in \mathcal{S}} \sum_{o \in \mathcal{O}} \lambda^{BEB} x_{oi}, \quad (61)$$

Eq. (61) is subject to (7)–(9). The binary variable x_{ij} is determined, and then, the binary variable comes to the second problem as a parameter. In the second step of the problem, the following problem is solved.

$$\min \sum_{t \in \mathcal{T}} \sum_{w \in \mathcal{W}} \sum_{b \in \mathcal{B}} \rho_w \left(\lambda_{t,w}^M p_{b,w,t} + \sum_{g \in \mathcal{G}} C_{g,t,w}^{EQ} + PF \cdot \Delta V_{b,w,t} \right), \quad (62)$$

$$V_{b,w,t} \geq \underline{V} - \Delta V_{b,w,t}, \quad \forall b \in \mathcal{B}, w \in \mathcal{W}, t \in \mathcal{T}, \quad (63)$$

where the bilinear product is substituted with the equivalent linear term in (60). Since the scheduling of BEBs adheres to a timetable, the charging demands may result in infeasible voltage bounds. Therefore, considering the feasibility concerns, we substitute the lower bound of the voltage constraint with a penalty term in the objective function at the upper-level. The amount of the penalty is contingent upon the degree of voltage violation, which is calculated in (63). It is important to note that setting a fixed lower bound for voltage may lead to power flow infeasibility under high charging demands. To address this, the penalty term is designed to penalize infeasible solutions, guiding them towards reduced infeasibility while simultaneously allowing a degree of freedom for certain violations. The modified upper-level objective function is subject to the constraints of BEB transit system, APDN, and lower-level problem, including (10)–(23), (25)–(32), (37)–(40), (42)–(44), (50)–(60), and (63).

5. Numerical experiments and results

This section presents a case study about optimization of the coupled BEB transit system and APDN system utilizing the proposed methods. Our study delves into the impact of the BEB transit system on the PDN and then deploys the flexibility of the DR to mitigate the adverse effects of charging demands from BEBs on the PDN in terms of obtained voltage from the power flow model.

5.1. Case study

The case study uses a sub-transit BEB system in Skövde, Sweden, and 33-node APDN towards demonstrating the effectiveness of the proposed methods. The sub-transit BEB system includes five terminals, while three of them are connected to the APDN at the nodes #5, #19, and #31 with a nominal charging capacity of 600 kW, 300 kW, and 600 kW, respectively. There is a depot with the capability of charging BEBs connected to the APDN #7 with a capacity of 400 kW. The depot is situated at the APDN node #7. There are three routes in the BEB sub-transit system depicted in Fig. 2 based on real information from Västtraffik (2023), with the length of 9.1, 14, 6.4 km, for routes #1, #2, and #3, respectively. The timetables comprise a total of 833 trips across the three routes mentioned. However, we have merged some trips to alleviate the computational burden when there is no possibility of charging between two consecutive trips. The threshold for deciding whether to merge the trips is whether the time gap between two service trips is over 5 min. Following the merging process, 316 trips are obtained. The first trip commences at 04:50, and the last trip ends at 23:58. The battery capacity of the BEBs is homogeneous, with each BEB equipped with a 300 kWh battery, as reported by Gao et al. (2017). The active and reactive peak demands in the PDN (excluding the charging demands of the BEBs) are 3700 kW and 1800 kVar, respectively.

The characteristics of the demands and impedance of the PDN are adopted from Najafi et al. (2020). The electricity prices and electricity demands data are sourced from Homaee et al. (2023). The mean value of PV generations is adopted from Najafi et al. (2020). The uncertainty of the electricity prices and PV generations are addressed through stochastic programming by generating four scenarios for each uncertainty source with the given mean values and 10% standard deviation deploying a normal distribution function. The combination of scenarios results in a total of 16 scenarios considering the capabilities of our operating system and without loss of generality.

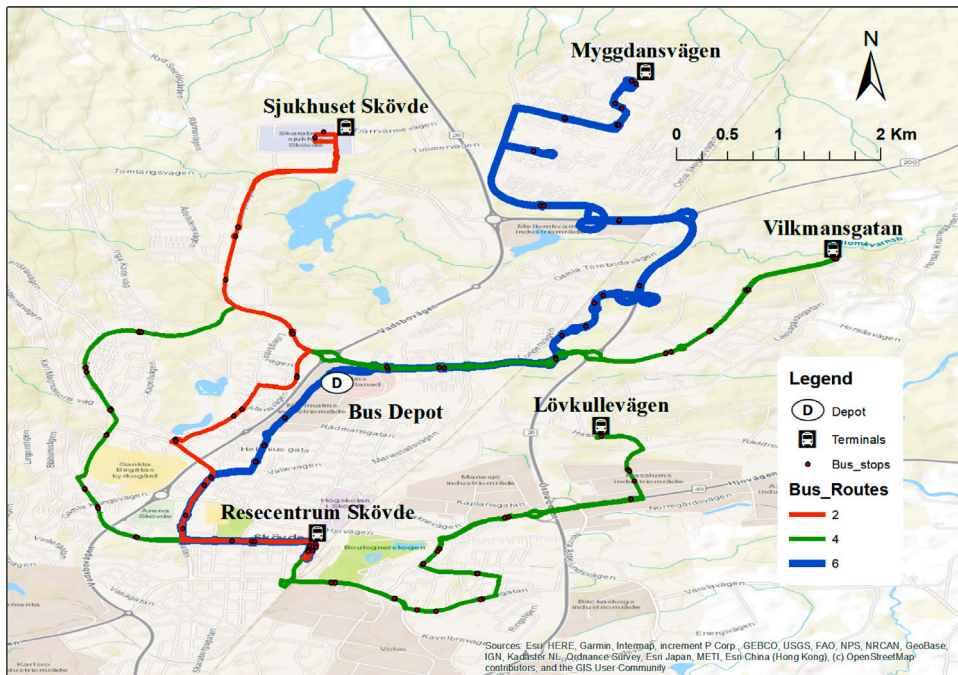


Fig. 2. Routes under study in the city of Skövde.

Table 2
Characteristics of the case study.

Item	value
PV capacity in each location (kW)	300
Total lengths of three routes (km)	29.5
BEB battery capacity (kWh)	300
Energy consumption rate of BEBs (kWh/km)	1.67
Minimum/maximum level of energy of BEBs	20%, 90%
Total initial active demands of APDN (kW)	3700
Total initial reactive demands of APDN (kVar)	1800
Maximum capacity of chargers in each station (kW)	600

The scenarios of electricity prices and PV generations along with the pattern of electricity demands, are shown in Figs. 3 and 4. The operation horizon is 24-h with a resolution of every two minutes. It should be noted that the timetable resolution of the BEB system is one-minute, but we have decreased the resolution to each two-minute as the time sample to reduce the computational burden without sacrificing the generality of the problem. The output voltage of the PDN nodes should adhere to the minimum bound of 0.9 pu and the upper limit of 1.05 pu. The energy consumption of BEBs is assumed to be 1.67 kWh per kilometer, and the average speed is 30 km/h. The minimum and maximum levels of the energy of the BEBs are set at 20% and 90%, respectively. The maximum electrical demand is situated at node #25 of the PDN, where the demand reaches 420 kW. Thus, we presume that the maximum charging capacity of a station for BEBs is 600 kW, taking into account other electrical demands within the PDN. However, this capacity may vary in other cases. The characteristics of the capacities and BEBs are summarized in Table 2. There are three DR aggregators, where APDN nodes #1–#22, #23–#25, and #26–#33 are managed by aggregator #1, #2, and #3, respectively. It is assumed that a maximum of 15% of the electricity of consumers can be curtailed (or shifted), while the power curtailment at each hour cannot exceed 25% of the initial demand at that hour. The simulations are performed on GAMS under a CPLEX solver utilizing a Ci5 laptop equipped with 16 GB RAM for solving the proposed second-order conic problem.

5.2. Results and discussion

After optimization, 10 BEBs are scheduled to cover 316 trips over a 24-h period. Fig. 5 exhibits the results of trip assignment to the electric BEBs. We take the trip chains of BEBs #5 and #6 for explanations. Bus #5 initiates the trips on route #2 by serving two trips before transitioning to route #1 for the subsequent three trips. On the other hand, bus #6 commences the first two trips on route #3 followed by a transition to route #2. Fig. 6 depicts the level of energy for BEBs #5 and #6. Both of the BEBs start the trip when they are fully charged (or near fully charged). These BEBs are charged en-route multiple times to support the energy

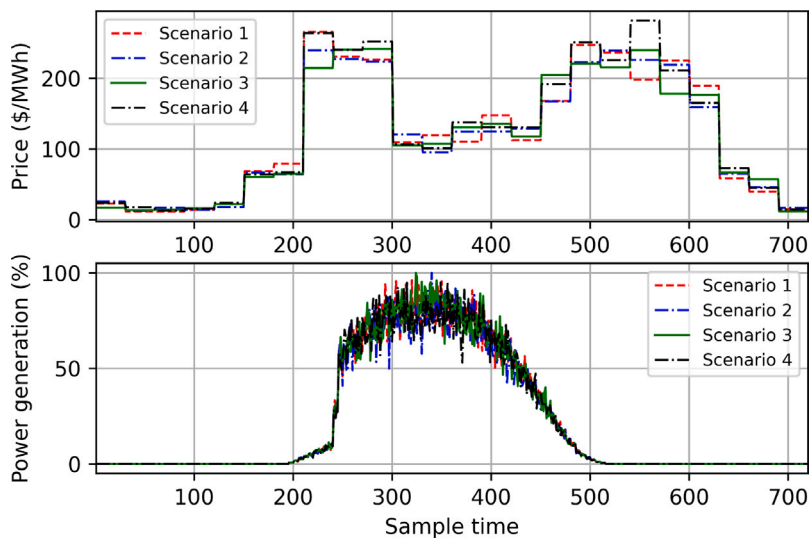


Fig. 3. Generated scenarios of electricity prices and PV productions.

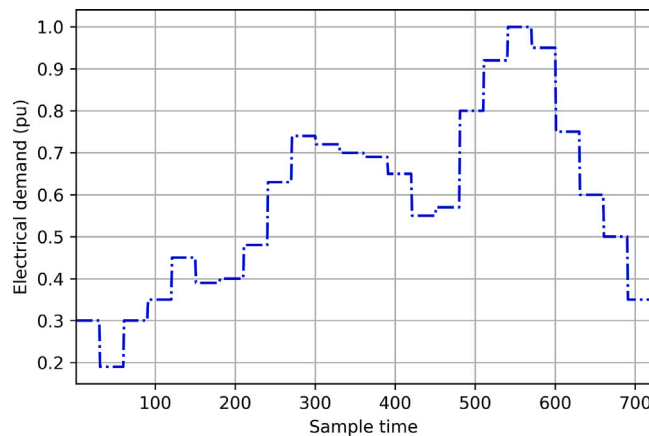


Fig. 4. Pattern of existing electricity demands on the PDN.

consumption during the trips. However, upon finishing their final trips, both BEBs return to the depot with low energy levels, thus facilitating the opportunity for recharging during the period of low electricity prices, typically occurring between 00:00 and 08:00, as depicted in Fig. 3).

The bars within Fig. 6 represent the received charging energy when the electric BEBs undergo recharging after a trip. For example, bus #6 is charged after trips #59, #68, and #75, and the energy level curve reveals an increase after charging. Obviously, the higher the charged energy is, the higher the slope of curve is. In addition, Fig. 7 graphically depicts the time intervals and charging amounts at bus stations (en-route). The vertical axis represents the deployed BEBs, while the horizontal axis corresponds to the time samples. The charged energy is illustrated by the intensity of the color displayed on the right bar, which ranges from 0 to 40 kWh. Darker colors represent higher charging energy received by the BEBs. Each box represents a charging activity, and the width of the boxes indicates the duration of the charging activity including starting and ending timestamps. For instance, BEB#1 charges in the time intervals of #172–#176, #335–#342, #375–#376, #385–#387, #414, #595–#609, #648–#662, and #670–#684. It is observed that during peak hours (after timeslot 500), the charging duration of the BEBs is longer compared to off-peak hours. However, the charging energy received is lower, resulting in reduced charging demand during peak hours, as shown in Fig. 8. The reasons for this reduced charging demand during peak hours are explored further from the PDN perspective, particularly considering its impact on output voltage. Aligned with the level of energy and received charged energy by the BEBs, Fig. 8 demonstrates the gathered charging demands of BEBs during the operational horizon in the depot and en-route. The overall charging demand is the accumulative value of the two graphs in the figure. The highest charging demands are in the early-morning hours prior to time slot #100 (one timeslot is 2 min), when BEBs are charged at the depot to take advantage of lower electricity prices. However, the charging demands during other hours (en-route charging) exhibit lower magnitudes. It is worth mentioning that the lowest charging demands are during time

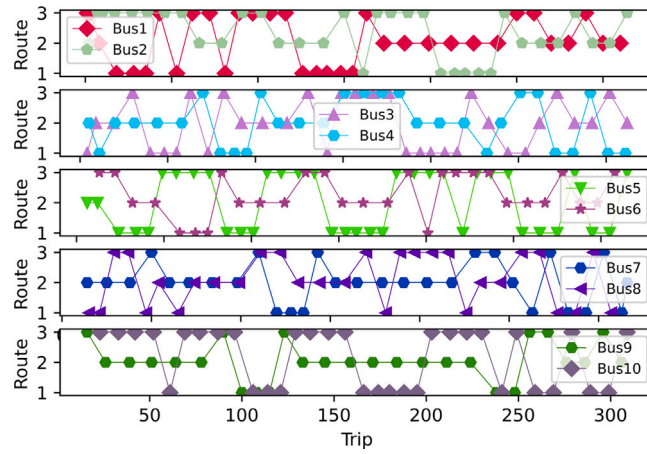


Fig. 5. Distribution of BEBs to support the trips.

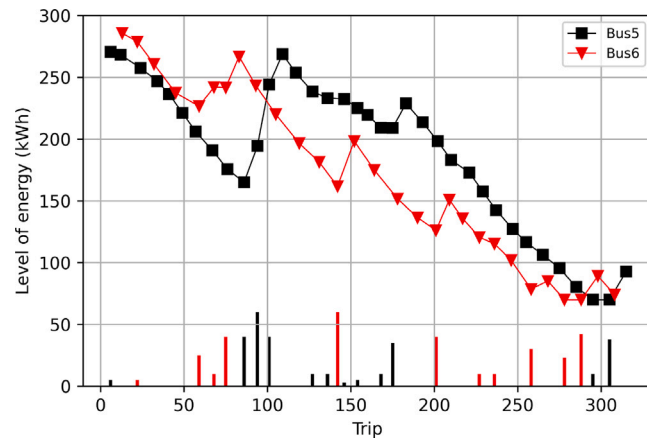


Fig. 6. Variation of level of energy of BEBs with respect to the trips.

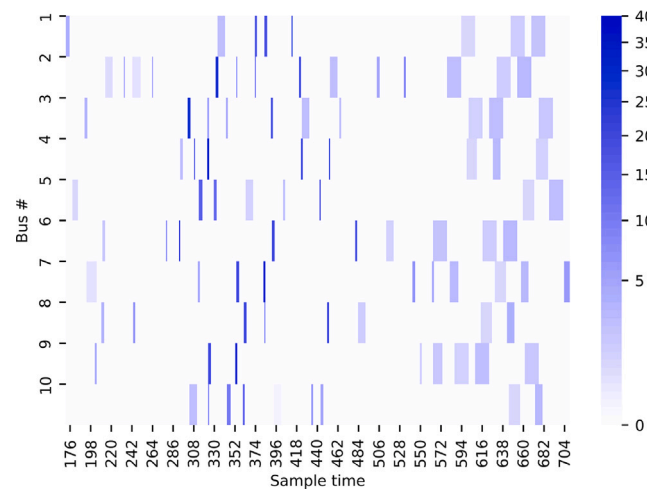


Fig. 7. Duration and charging time, charging value (in kWh) of the BEBs on bus stations (en-route).

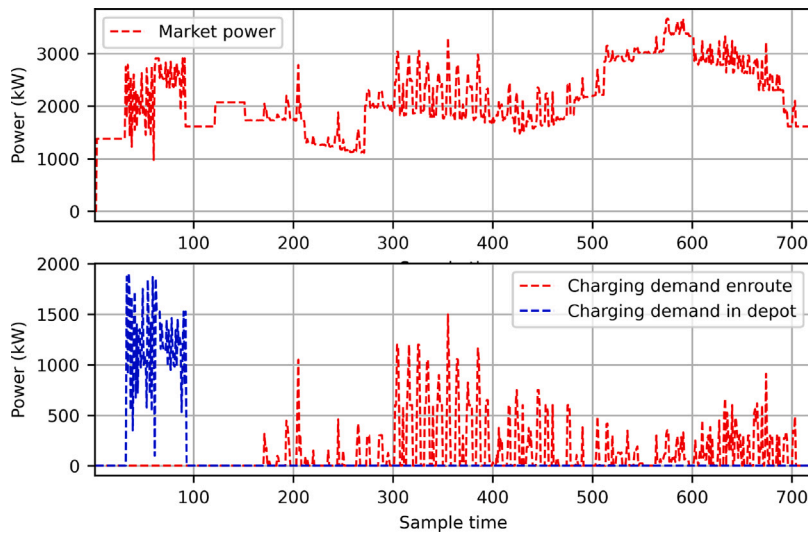


Fig. 8. Electricity purchased from the market and charging demands of BEBs.

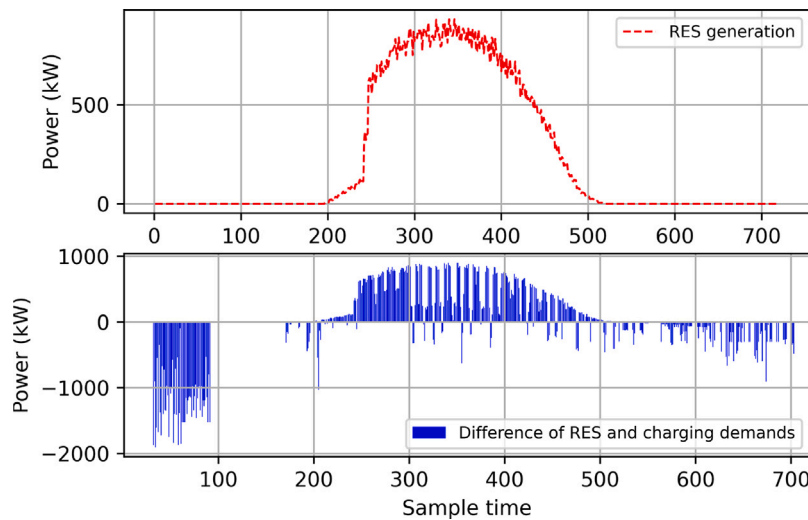


Fig. 9. Temporal PV generations and supports of the PDN.

samples #500 to #600, coinciding with the peak of the electricity demands from other sectors and electricity prices. The en-route charging starts after sample time 170 which is equivalent to 05:40 in the morning. It should be noted that the first trip is at 04:50.

Electricity purchased from the market in Fig. 8 also underscores the burden of charging demands from BEB on the PDN by adding a fluctuation to the initial electricity demands of the PDN (as shown in Fig. 4). Importantly, these charging demands from BEBs create another peak in the early-morning hours, while it does not pose a significant challenge to the APDN. This is because the depot is located in a less vulnerable place of the PDN (PDN node #5), which can host higher demands within the APDN. Fig. 9 shows the generation of PVs alongside the difference between charging demands and electricity from PV generations. The negative values in the early-morning hours denote that the electricity from PVs are insufficient to support the charging demands of BEBs. During the day and mostly for the en-rout charging, the required electricity for charging demands of BEBs can be supported by the PVs. However, a notable portion of electricity from the power grid are needed in the depot to charge BEBs during early-morning hours.

Fig. 10 yields the results of activating the DR service in the APDN. The load curtailment is executed during peak hours spanning from time samples #451 to #600, and #211 to #270 aligning with the peak of electricity prices and demands. The curtailed loads are subsequently shifted to other time intervals characterized by lower electricity prices, thereby mitigating overall electricity procurement costs. However, the shifted electricity is dispersed across various hours, rather than solely concentrated in the cheapest time slots. Indeed, the cheapest time coincides with the new electricity demand peak due to the charging demands of BEBs,

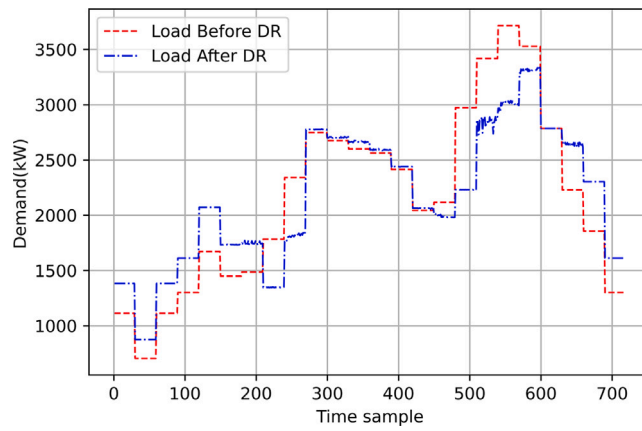


Fig. 10. Results of the total DR compared to the input electrical demand.

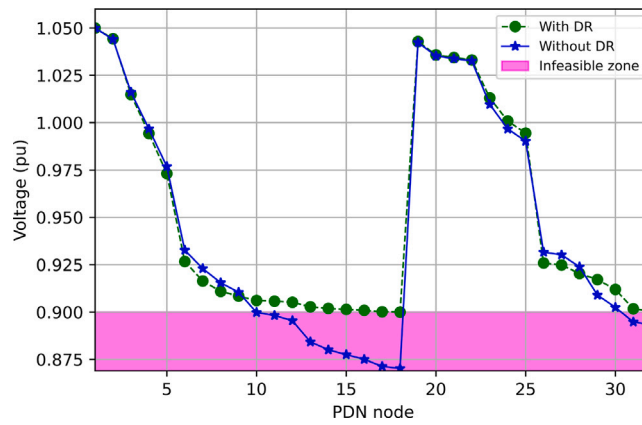


Fig. 11. Minimum obtained voltage over all times and scenarios.

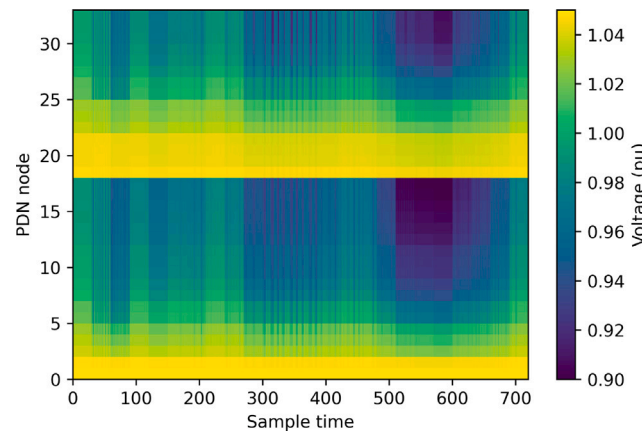


Fig. 12. Obtained voltage over all times and scenarios.

precluding further demand increase. Additionally, the results indicate that all curtailed electricity during peak hours is shifted to the off-peak hours, showing that the amount of electricity not supplied during the activation of DR is zero.

Further insights into the coordination between charging scheduling of BEBs and DR flexibility are provided in Fig. 11. Even though a significant portion of the charging demands from BEBs are not scheduled during peak hours, the minimum level of the output voltage of the PDN is violated when the DR service is not activated as shown by the blue curve in Fig. 11. The minimum

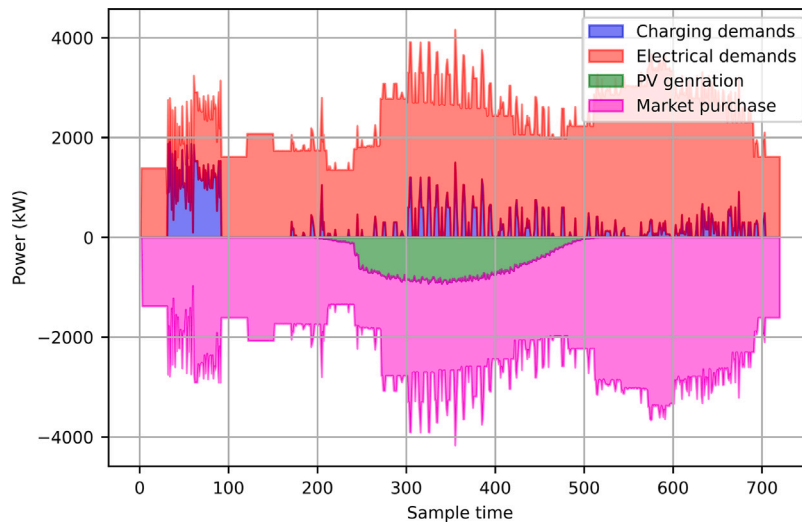


Fig. 13. Balance of the generation and consumption in the PDN.

Table 3

Summarized results for the upper and lower levels.

Item	value
Upper-level cost (\$)	21 062
DR Aggregator profit (\$)	1550
Electricity market cost (\$)	19 512
Average of load curtailment (kWh)	139.7
Average of load shift (kWh)	139.7
Not supplied electricity (kWh)	0

voltage in PDN is elevated by activating the DR service to meet the minimum allowable bound of the voltage by curtailing 3352 kWh of the energy and shifting to the other hours. It should be noted that the total energy without activating the DR excluding the charging demand from BEBs, is 51935 kWh. The curtailed electrical energy (which is thoroughly shifted) is equal to 6.4% of the initial demands in kWh. This declares that the curtailment of the electricity demands during peak hours can effectively compensate for the en-route charging demands of BEBs during peak hours. Fig. 12 depicts the expected value of the voltage across all time slots when DR is utilized. All obtained voltages are above 0.9 pu, showing the reliability of the results in meeting the output voltage of the APDN. It can also be observed from the figure that APDN nodes #13–#18 and #28–#33 are the most critical nodes during the peak time samples #500–#600, as they yield the lowest expected voltage. Referring to Fig. 7, the reduced charging depth after timeslot #500 can be attributed to the vulnerability of the PDN during these hours. As the charging demand (in terms of power) increases, the voltage level decreases. Consequently, the duration of en-route charging extends instead of increasing the magnitude of the charge. It is important to note that the case study used for the APDN represents a healthy network capable of maintaining a minimum voltage level of 0.9 pu before the addition of new demands. However, this outcome may vary depending on the specific case. The initial condition of the APDN plays a crucial role; some networks can accommodate higher charging demands, while others may be more vulnerable. Consequently, decisions regarding flexibility must account for the varying vulnerability and stability of the network when subjected to new charging demands.

Fig. 13 shows the balance between electricity procured and consumed in each time sample. The positive values denote electricity consumption, while the negative values indicate electricity procurement. It is apparent that the primary source of electricity procurement is purchased from the electricity market. Additionally, some part of the electricity is supplied through the PV generations in the middle of the day. The electricity demands from other sectors on the PDN are the main load of the PDN. Nevertheless, the charging demands from BEBs add some demands in other hours, particularly in the early-morning hours when the BEBs are charged at the depot. Finally, we summarize the obtained results for the cost of the upper and lower levels, as well as the curtailed and shifted electricity in Table 3. The upper-level cost includes the electricity market cost and the cost of operating DR aggregators. The average curtailment and shift loads indicate the average over the scheduling period (24 h). The equality of the curtailment and the shift (139.78 kWh) verifies that the supplied electricity demand is zero, i.e. balanced electricity supply and demand.

6. Conclusion

This study presents a novel optimization framework designed for the efficient management of a coupled BEB transit system and APDN. The framework addresses the joint optimization of operational scheduling of BEBs (operation and charging scheduling) and

the integration of demand response services in the APDN to satisfy the charging demand of BEBs without violating the voltage constraints of APDN. The objective is to minimize the total cost of fleet of BEBs and electricity procurement to appropriately meet charging demands of BEBs and electricity demand from other sectors. A case study in Skövde, Sweden is conducted to demonstrate the proposed methods. The results reveal the appropriate assignment of electric buses to fit the service trips of bus timetables as well as the proper charging scheduling with minimal costs. The charging of BEBs is concentrated in the depot in order to benefit from lower electricity prices. Although this results in another electricity demand peak in the morning due to the charging requirements of BEBs, the proximity of the depot to the source of the APDN mitigates associated challenges. Furthermore, the demand response service elevates the minimum voltage level by curtailing 3352 kWh of the electricity demands during the peak hours and shifting it to the other hours to avoid violation of power grid voltage due to charging demand from BEBs.

Even though our study has contributed to the literature on joint optimization of BEBs coupled with an active power distribution network integrated with DR flexibility, some future perspectives and challenges remain elusive. First, we have simplified the energy consumption of electric buses through a linear relation with respect to driving distance. However, an accurate estimation of energy consumption can enhance the understanding of BEB operational situation and the network topology. Therefore, future perspectives should try to explore energy consumption predictions with uncertainty (Jia et al., 2025b). Second, this study has overlooked battery degradation of BEBs. Degradation cost is an interesting topic and a challenge for researchers due to the intricacy of precise estimation of the degradation cost (Jia et al., 2025a). Hence, a possible future research direction includes a proper degradation approach to our proposed framework, promising a more comprehensive optimization. Lastly, the DR program has been introduced to reduce the burden of charging demands from BEBs on APDN. However, there is another potential within APDN to mitigate the impact of charging demands. It is a promising and worthy future direction to further explore the combination of improving both generation and demand sides simultaneously to cope with the additional charging demands and various uncertainties in both BEB transit and APDN system.

CRedit authorship contribution statement

Arsalan Najafi: Writing – review & editing, Writing – original draft, Project administration, Methodology, Investigation, Conceptualization. **Kun Gao:** Writing – review & editing, Validation, Supervision, Project administration, Funding acquisition, Formal analysis, Conceptualization. **Hua Wang:** Writing – review & editing, Methodology, Formal analysis. **Michal Jasinski:** Writing – review & editing, Methodology, Formal analysis. **Omkar Parishwad:** Writing – review & editing, Writing – original draft, Formal analysis. **Shaohua Cui:** Writing – review & editing, Investigation, Conceptualization. **Xiaohan Liu:** Formal analysis, Writing – review & editing.

Declaration of competing interest

The authors declare that they have no known competing financial interests or personal relationships that could have appeared to influence the work reported in this paper.

Acknowledgments

The research is supported by the research grant from National Natural Science Foundation Council of China (No. 72471070), JPI Urban Europe and Energimyndigheten (e-MATS, P2023-00029) and Area of Advance Transport at Chalmers University of Technology. Any opinions, findings, and conclusions or recommendations expressed in this paper are those of the authors and do not necessarily reflect the views of the sponsors.

Data availability

Data will be made available on request.

References

- Avishan, F., Yanikoğlu, İ., Alwesabi, Y., 2023. Electric bus fleet scheduling under travel time and energy consumption uncertainty. *Transp. Res. Part C: Emerg. Technol.* 156, 104357. <http://dx.doi.org/10.1016/j.trc.2023.104357>, URL: <https://www.sciencedirect.com/science/article/pii/S0968090X23003479>.
- Bahlawan, H., Castorino, G.A.M., Losi, E., Manservigi, L., Spina, P.R., Venturini, M., 2022. Optimal management with demand response program for a multi-generation energy system. *Energy Convers. Manag.* 16, 100311. <http://dx.doi.org/10.1016/j.ecmx.2022.100311>, URL: <https://www.sciencedirect.com/science/article/pii/S2590174522001349>.
- Bao, Z., Li, J., Bai, X., Xie, C., Chen, Z., Xu, M., Shang, W.-L., Li, H., 2023. An optimal charging scheduling model and algorithm for electric buses. *Appl. Energy* 332, 120512. <http://dx.doi.org/10.1016/j.apenergy.2022.120512>, URL: <https://www.sciencedirect.com/science/article/pii/S030626192201769X>.
- Baran, M., Wu, F., 1989. Network reconfiguration in distribution systems for loss reduction and load balancing. *IEEE Trans. Power Deliv.* 4 (2), 1401–1407. <http://dx.doi.org/10.1109/61.25627>.
- Carrion, M., Arroyo, J.M., Conejo, A.J., 2009. A bilevel stochastic programming approach for retailer futures market trading. *IEEE Trans. Power Syst.* 24 (3), 1446–1456. <http://dx.doi.org/10.1109/TPWRS.2009.2019777>.
- Cui, S., Gao, K., Yu, B., Ma, Z., Najafi, A., 2023. Joint optimal vehicle and recharging scheduling for mixed bus fleets under limited chargers. *Transp. Res. Part E: Logist. Transp. Rev.* 180, 103335. <http://dx.doi.org/10.1016/j.trre.2023.103335>, URL: <https://www.sciencedirect.com/science/article/pii/S136655452300323X>.

- Dong, G., Witlox, F., Bie, Y., 2024. Decentralizing e-bus charging infrastructure deployment leads to economic and environmental benefits. *Commun. Transp. Res.* 4, 100139. <http://dx.doi.org/10.1016/j.commtr.2024.100139>, URL: <https://www.sciencedirect.com/science/article/pii/S2772424724000222>.
- Duan, M., Liao, F., Qi, G., Guan, W., 2023. Integrated optimization of electric bus scheduling and charging planning incorporating flexible charging and timetable shifting strategies. *Transp. Res. Part C: Emerg. Technol.* 152, 104175. <http://dx.doi.org/10.1016/j.trc.2023.104175>, URL: <https://www.sciencedirect.com/science/article/pii/S0968090X2300164X>.
- El-Taweel, N.A., Farag, H.E.Z., Mohamed, M., 2020. Integrated utility-transit model for optimal configuration of battery electric bus systems. *IEEE Syst. J.* 14 (1), 738–748. <http://dx.doi.org/10.1109/JSYST.2019.2926460>.
- Gao, Z., Lin, Z., LaClair, T.J., Liu, C., Li, J.-M., Birky, A.K., Ward, J., 2017. Battery capacity and recharging needs for electric buses in city transit service. *Energy* 122, 588–600. <http://dx.doi.org/10.1016/j.energy.2017.01.101>, URL: <https://www.sciencedirect.com/science/article/pii/S0360544217301081>.
- Guschinsky, N., Kovalyov, M.Y., Pesch, E., Rozin, B., 2023. Cost minimizing decisions on equipment and charging schedule for electric buses in a single depot. *Transp. Res. Part E: Logist. Transp. Rev.* 180, 103337. <http://dx.doi.org/10.1016/j.tre.2023.103337>, URL: <https://www.sciencedirect.com/science/article/pii/S1366554523003253>.
- Hartvigsson, E., Taljegard, M., Odenberger, M., Chen, P., 2022. A large-scale high-resolution geographic analysis of impacts of electric vehicle charging on low-voltage grids. *Energy* 261, 125180. <http://dx.doi.org/10.1016/j.energy.2022.125180>, URL: <https://www.sciencedirect.com/science/article/pii/S0360544222020710>.
- He, Y., Liu, Z., Song, Z., 2023. Joint optimization of electric bus charging infrastructure, vehicle scheduling, and charging management. *Transp. Res. Part D: Transp. Environ.* 117, 103653. <http://dx.doi.org/10.1016/j.trd.2023.103653>, URL: <https://www.sciencedirect.com/science/article/pii/S1361920923000500>.
- Homaee, O., Najafi, A., Jasinski, M., Tsaousoglou, G., Leonowicz, Z., 2023. Coordination of neighboring active distribution networks under electricity price uncertainty using distributed robust bi-level programming. *IEEE Trans. Sustain. Energy* 14 (1), 325–338. <http://dx.doi.org/10.1109/TSTE.2022.3212004>.
- Huang, D., Zhang, J., Liu, Z., 2023. A robust coordinated charging scheduling approach for hybrid electric bus charging systems. *Transp. Res. Part D: Transp. Environ.* 125, 103955. <http://dx.doi.org/10.1016/j.trd.2023.103955>, URL: <https://www.sciencedirect.com/science/article/pii/S1361920923003528>.
- Jia, R., Gao, K., Cui, S., Chen, J., Andric, J., 2025a. A multi-objective reinforcement learning-based velocity optimization approach for electric trucks considering battery degradation mitigation. *Transp. Res. Part E: Logist. Transp. Rev.* 194, 103885. <http://dx.doi.org/10.1016/j.tre.2024.103885>, URL: <https://www.sciencedirect.com/science/article/pii/S1366554524004769>.
- Jia, R., Gao, K., Liu, Y., Yu, B., Ma, X., Ma, Z., 2025b. I-CLTP: Integrated contrastive learning with transformer framework for traffic state prediction and network-wide analysis. *Transp. Res. Part C: Emerg. Technol.* 171, 104979. <http://dx.doi.org/10.1016/j.trc.2024.104979>, URL: <https://www.sciencedirect.com/science/article/pii/S0968090X2400500X>.
- Li, B., Chen, Y., Wei, W., Huang, S., Mei, S., 2021. Resilient restoration of distribution systems in coordination with electric bus scheduling. *IEEE Trans. Smart Grid* 12 (4), 3314–3325. <http://dx.doi.org/10.1109/TSG.2021.3060801>.
- Li, W., He, Y., Hu, S., He, Z., Ratti, C., 2024. Planning dynamic wireless charging infrastructure for battery electric bus systems with the joint optimization of charging scheduling. *Transp. Res. Part C: Emerg. Technol.* 159, 104469. <http://dx.doi.org/10.1016/j.trc.2023.104469>, URL: <https://www.sciencedirect.com/science/article/pii/S0968090X2300459X>.
- Li, J., Xu, X., Yan, Z., Wang, H., Shahidepour, M., Chen, Y., 2023. Coordinated optimization of emergency response resources in transportation-power distribution networks under extreme events. *IEEE Trans. Smart Grid* <http://dx.doi.org/10.1109/TSG.2023.3257040>, 1–1.
- Lin, Y., Zhang, K., Shen, Z.-J.M., Ye, B., Miao, L., 2019. Multistage large-scale charging station planning for electric buses considering transportation network and power grid. *Transp. Res. Part C: Emerg. Technol.* 107, 423–443. <http://dx.doi.org/10.1016/j.trc.2019.08.009>, URL: <https://www.sciencedirect.com/science/article/pii/S0968090X18312105>.
- Low, S.H., 2014. Convex relaxation of optimal power flow—Part II: Exactness. *IEEE Trans. Control. Netw. Syst.* 1 (2), 177–189.
- Mohamed, M., Farag, H., El-Taweel, N., Ferguson, M., 2017. Simulation of electric buses on a full transit network: Operational feasibility and grid impact analysis. *Electr. Power Syst. Res.* 142, 163–175. <http://dx.doi.org/10.1016/j.epr.2016.09.032>, URL: <https://www.sciencedirect.com/science/article/pii/S0378779616303959>.
- Najafi, A., Homaee, O., Jasiński, M., Tsaousoglou, G., Leonowicz, Z., 2023. Integrating hydrogen technology into active distribution networks: The case of private hydrogen refueling stations. *Energy* 278, 127939. <http://dx.doi.org/10.1016/j.energy.2023.127939>, URL: <https://www.sciencedirect.com/science/article/pii/S0360544223013336>.
- Najafi, A., Masoudian, A., Mohammadi-Ivatloo, B., 2020. Optimal capacitor placement and sizing in distribution networks. In: Pesaran Hajiabbas, M., Mohammadi-Ivatloo, B. (Eds.), *Optimization of Power System Problems: Methods, Algorithms and MATLAB Codes*. Springer International Publishing, Cham, pp. 75–101. http://dx.doi.org/10.1007/978-3-030-34050-6_4.
- Najafi, A., Pourakbari-Kasmaei, M., Contreras, J., Lehtonen, M., Leonowicz, Z., 2022. Optimal bilevel operation-planning framework of distributed generation hosting capacity considering rival DISCO and EV aggregator. *IEEE Syst. J.* 16 (3), 5023–5034. <http://dx.doi.org/10.1109/JSYST.2021.3123242>.
- Najafi, A., Tsaousoglou, G., Gao, K., Parishwad, O., 2024. Coordination of coupled electrified road systems and active power distribution networks with flexibility integration. *Appl. Energy* 369, 123546. <http://dx.doi.org/10.1016/j.apenergy.2024.123546>, URL: <https://www.sciencedirect.com/science/article/pii/S0306261924009292>.
- Perumal, S.S., Lusby, R.M., Larsen, J., 2022. Electric bus planning & scheduling: A review of related problems and methodologies. *European J. Oper. Res.* 301 (2), 395–413. <http://dx.doi.org/10.1016/j.ejor.2021.10.058>, URL: <https://www.sciencedirect.com/science/article/pii/S03772217211009140>.
- Qiao, W., Han, Y., Zhao, Q., Si, F., Wang, J., 2022. A distributed coordination method for coupled traffic-power network equilibrium incorporating behavioral theory. *IEEE Trans. Veh. Technol.* 71 (12), 12588–12601. <http://dx.doi.org/10.1109/TVT.2022.3206095>.
- Ren, H., Ma, Z., Ming Lun Fong, A., Sun, Y., 2022. Optimal deployment of distributed rooftop photovoltaic systems and batteries for achieving net-zero energy of electric bus transportation in high-density cities. *Appl. Energy* 319, 119274. <http://dx.doi.org/10.1016/j.apenergy.2022.119274>, URL: <https://www.sciencedirect.com/science/article/pii/S03062619220006316>.
- Shaheen, A., Elsayed, A., El-Schiemy, R.A., Abdelaziz, A.Y., 2021. Equilibrium optimization algorithm for network reconfiguration and distributed generation allocation in power systems. *Appl. Soft Comput.* 98, 106867. <http://dx.doi.org/10.1016/j.asoc.2020.106867>, URL: <https://www.sciencedirect.com/science/article/pii/S156849462030805X>.
- Shao, C., Li, K., Qian, T., Shahidepour, M., Wang, X., 2023. Generalized user equilibrium for coordination of coupled power-transportation network. *IEEE Trans. Smart Grid* 14 (3), 2140–2151. <http://dx.doi.org/10.1109/TSG.2022.3206511>.
- Sivasankari, G., Narayanan, K., 2022. Demand response approach in the presence of plug-in hybrid electric vehicle for profit maximization of utility. *Energy Convers. Manag.* 15, 100263. <http://dx.doi.org/10.1016/j.ecmx.2022.100263>, URL: <https://www.sciencedirect.com/science/article/pii/S2590174522000861>.
- Västrafrik, 2023. Västrafrik. Available at: <https://www.vastrafrik.se>.
- Wang, S., Chen, S., Ge, L., Wu, L., 2016. Distributed generation hosting capacity evaluation for distribution systems considering the robust optimal operation of OLTC and SVC. *IEEE Trans. Sustain. Energy* 7 (3), 1111–1123. <http://dx.doi.org/10.1109/TSTE.2016.2529627>.
- Wang, Y., Huang, Y., Xu, J., Barclay, N., 2017. Optimal recharging scheduling for urban electric buses: A case study in davis. *Transp. Res. Part E: Logist. Transp. Rev.* 100, 115–132. <http://dx.doi.org/10.1016/j.tre.2017.01.001>, URL: <https://www.scopus.com/inward/record.uri?eid=s2-s2.0-85014077734&doi=10.1016%2fj.tre.2017.01.001&partnerID=40&md5=8e76ec1bba95466c8afa18ca65407a1d>, Cited by: 198.

- Wang, X., Song, Z., Xu, H., Wang, H., 2023. En-route fast charging infrastructure planning and scheduling for battery electric bus systems. *Transp. Res. Part D: Transp. Environ.* 117, 103659. <http://dx.doi.org/10.1016/j.trd.2023.103659>, URL: <https://www.sciencedirect.com/science/article/pii/S1361920923000561>.
- Wen, L., Zhou, K., Feng, W., Yang, S., 2024. Demand side management in smart grid: A dynamic-price-based demand response model. *IEEE Trans. Eng. Manage.* 71, 1439–1451. <http://dx.doi.org/10.1109/TEM.2022.3158390>.
- Wu, C., Wang, T., Zhou, D., Cao, S., Sui, Q., Lin, X., Li, Z., Wei, F., 2023. A distributed restoration framework for distribution systems incorporating electric buses. *Appl. Energy* 331, 120428. <http://dx.doi.org/10.1016/j.apenergy.2022.120428>, URL: <https://www.sciencedirect.com/science/article/pii/S0306261922016853>.
- Xie, D.-F., Yu, Y.-P., Zhou, G.-J., Zhao, X.-M., Chen, Y.-J., 2023. Collaborative optimization of electric bus line scheduling with multiple charging modes. *Transp. Res. Part D: Transp. Environ.* 114, 103551. <http://dx.doi.org/10.1016/j.trd.2022.103551>, URL: <https://www.sciencedirect.com/science/article/pii/S1361920922003777>.
- Yi, Z., Xu, Y., Wang, H., Sang, L., 2021. Coordinated operation strategy for a virtual power plant with multiple DER aggregators. *IEEE Trans. Sustain. Energy* 12 (4), 2445–2458. <http://dx.doi.org/10.1109/TSTE.2021.3100088>.
- Zeng, Z., Wang, T., Qu, X., 2024. En-route charge scheduling for an electric bus network: Stochasticity and real-world practice. *Transp. Res. Part E: Logist. Transp. Rev.* 185, 103498. <http://dx.doi.org/10.1016/j.tre.2024.103498>, URL: <https://www.sciencedirect.com/science/article/pii/S1366554524000899>.
- Zhang, L., Han, Y., Peng, J., Wang, Y., 2023. Vehicle and charging scheduling of electric bus fleets: A comprehensive review. *J. Intell. Connect. Veh.* 6 (3), 116–124. <http://dx.doi.org/10.26599/JICV.2023.9210012>.
- Zhang, M., Yang, M., 2024. Optimal electric bus scheduling considering battery degradation effect and charging facility capacity. *Transp. Lett.* 1–11. <http://dx.doi.org/10.1080/19427867.2024.2363659>, arXiv:<https://doi.org/10.1080/19427867.2024.2363659>.
- Zhao, H., Wang, B., Pan, Z., Sun, H., Guo, Q., Xue, Y., 2021. Aggregating additional flexibility from quick-start devices for multi-energy virtual power plants. *IEEE Trans. Sustain. Energy* 12 (1), 646–658. <http://dx.doi.org/10.1109/TSTE.2020.3014959>.
- Zhong, L., En, H.S., Pei, M., Xiong, J., Wang, T., 2024. Optimized speed control for electric vehicles on dynamic wireless charging lanes: An eco-driving approach. *J. Intell. Connect. Veh.* 7 (1), 52–63. <http://dx.doi.org/10.26599/JICV.2023.9210033>.
- Zhou, Y., Meng, Q., Ong, G.P., Wang, H., 2024a. Electric bus charging scheduling on a bus network. *Transp. Res. Part C: Emerg. Technol.* 161, 104553. <http://dx.doi.org/10.1016/j.trc.2024.104553>, URL: <https://www.sciencedirect.com/science/article/pii/S0968090X24000743>.
- Zhou, Y., Wang, H., Wang, Y., Yu, B., Tang, T., 2024b. Charging facility planning and scheduling problems for battery electric bus systems: A comprehensive review. *Transp. Res. Part E: Logist. Transp. Rev.* 183, 103463. <http://dx.doi.org/10.1016/j.tre.2024.103463>, URL: <https://www.sciencedirect.com/science/article/pii/S136655452400053X>.